

Aberystwyth University

Biogeochemical Connectivity Between Freshwater Ecosystems beneath the West Antarctic Ice Sheet and the Sub-Ice Marine Environment

Vick-Majors, Trista J.; Michaud, Alexander B.; Skidmore, Mark L.; Turetta, Clara; Barbante, Carlo; Christner, Brent C.; Dore, John E.; Christianson, Knut; Mitchell, Andrew C.; Achberger, Amanda M.; Mikucki, Jill A.; Priscu, John C.

Published in:
Global Biogeochemical Cycles

DOI:
[10.1029/2019GB006446](https://doi.org/10.1029/2019GB006446)

Publication date:
2020

Citation for published version (APA):
Vick-Majors, T. J., Michaud, A. B., Skidmore, M. L., Turetta, C., Barbante, C., Christner, B. C., Dore, J. E., Christianson, K., Mitchell, A. C., Achberger, A. M., Mikucki, J. A., & Priscu, J. C. (2020). Biogeochemical Connectivity Between Freshwater Ecosystems beneath the West Antarctic Ice Sheet and the Sub-Ice Marine Environment. *Global Biogeochemical Cycles*, 34(3), [e2019GB006446]. <https://doi.org/10.1029/2019GB006446>

General rights

Copyright and moral rights for the publications made accessible in the Aberystwyth Research Portal (the Institutional Repository) are retained by the authors and/or other copyright owners and it is a condition of accessing publications that users recognise and abide by the legal requirements associated with these rights.

- Users may download and print one copy of any publication from the Aberystwyth Research Portal for the purpose of private study or research.
- You may not further distribute the material or use it for any profit-making activity or commercial gain
- You may freely distribute the URL identifying the publication in the Aberystwyth Research Portal

Take down policy

If you believe that this document breaches copyright please contact us providing details, and we will remove access to the work immediately and investigate your claim.

tel: +44 1970 62 2400
email: is@aber.ac.uk

Biogeochemical connectivity between freshwater ecosystems beneath the West Antarctic Ice Sheet and the sub-ice marine environment

Trista J. Vick-Majors^{1,*}, Alexander B. Michaud^{2,‡}, Mark L. Skidmore³, Clara Turetta^{4,§}, Carlo Barbante^{4,5}, Brent C. Christner^{6,7}, John E. Dore², Knut Christianson⁸, Andrew C. Mitchell⁹, Amanda M. Achberger^{6§}, Jill A. Mikucki¹⁰, and John C. Prisco²

¹Department of Biological Sciences, Michigan Technological University, Houghton, MI, 49931 USA

²Department of Land Resources and Environmental Sciences, Montana State University, Bozeman, MT, 59717, USA

³Department of Earth Sciences, Montana State University, Bozeman, MT, 59717, USA

⁴Institute for the Dynamics of Environmental Processes – CNR, Venice 30123, Italy

⁵Department of Environmental Sciences, Informatics and Statistics, Ca' Foscari University of Venice, Venice 30123, Italy

⁶Department of Biological Sciences, Louisiana State University, Baton Rouge, LA, 70803, USA

⁷Department of Microbiology and Cell Science, Biodiversity Institute, University of Florida, Gainesville, FL, 32611, USA

⁸Department of Earth and Space Sciences, University of Washington, Seattle, WA, 98195, USA

⁹Department of Geography and Earth Sciences, Aberystwyth University, Aberystwyth, SY23 3DB, UK

¹⁰Department of Microbiology, University of Tennessee, Knoxville, TN, 37996, USA

*Corresponding author: Trista J. Vick-Majors (tjvickma@mtu.edu)

‡Present Address: Bigelow Laboratory for Ocean Sciences, East Boothbay, ME, 04544

§Present Address: Department of Oceanography, Texas A&M University, College Station, TX, 77843-3146, USA

§ Present Address: Institute of Polar Sciences, CNR, Venice 30123, Italy

Key Points:

- A mass balance shows that dissolved organic carbon accumulation in Whillans Subglacial Lake is under hydrological and biological control.
- Differences between the character of water column and sediment porewater dissolved organic matter imply biological processing.
- Subglacial outflows have the potential to subsidize biological activity under the world's largest ice shelf.

Abstract

Although subglacial aquatic environments are widespread beneath the Antarctic ice sheet, subglacial biogeochemistry is not well-understood and the contribution of subglacial water to coastal ocean carbon and nutrient cycling remains poorly constrained. The Whillans Subglacial Lake (SLW) ecosystem is upstream from West Antarctica's Gould-Siple Coast ~800 m beneath the surface of the Whillans Ice Stream. SLW hosts an active microbial ecosystem and is part of an active hydrological system that drains into the marine cavity beneath the adjacent Ross Ice Shelf. Here we examine sources and sinks for organic matter in the lake and estimate the freshwater carbon and nutrient delivery from discharges into the coastal embayment. Fluorescence-based characterization of dissolved organic matter (DOM) revealed microbially-driven differences between sediment pore waters and lake water, with an increasing contribution from relict humic-like DOM with sediment depth. Mass balance calculations indicated that the pool of dissolved organic carbon (DOC) in the SLW water column could be produced in 4.8 to 11.9 years, which is a time frame similar to that of the lakes' fill-drain cycle. Based on these estimates, subglacial lake water discharged at the Siple Coast could supply an average of 5,400% more than the heterotrophic demand within Siple Coast embayments (6.5% for the entire Ross Ice Shelf cavity). Our results suggest that subglacial discharge represents a heretofore unappreciated source of microbially-processed DOC and other nutrients to the Southern Ocean.

Plain Language Summary

Antarctica's thick ice sheets cover a continent rich with liquid water. These subglacial aquatic environments are home to microbial ecosystems that process organic matter and nutrients important for all life. At the same time, subglacial water in Antarctica actively flows between basins and from subglacial basins to the edge of the continent where it mixes with seawater in coastal areas covered by ice shelves. The waters under these ice shelves are cold, dark, and contain low concentrations of organic carbon and nutrients. We used data from Whillans Subglacial Lake, which lies 800 m beneath the ice of West Antarctica, to understand the sources, sinks, and accumulation of organic matter in Antarctic subglacial aquatic environments. We then combined data from the same lake with data on subglacial hydrology in the region to determine whether inputs of subglacial organic matter and nutrients could be important in supporting life in the dark waters beneath the adjacent ice shelf. We found that the input of freshwater from the Antarctic continent to the surrounding ocean can meet the microbial demand for organic carbon and nutrients under the ice shelf. This work has implications for our understanding of Antarctica's influence on biology in the Southern Ocean.

1 Introduction

The transport of terrestrially-derived carbon to coastal environments is a major pathway in the global carbon cycle (Bauer et al., 2013). Riverine fluxes have long been recognized as an important source of carbon and nutrients to the oceans (Meybeck 1982), with high fluxes of dissolved organic carbon (DOC) occurring at low latitudes (0 – 30°; 62% of total known global inputs) and northern high latitudes (60 – 90°; 19%) (Dai et al., 2012). Polar ice sheets and glaciers, which store ~70% of the Earth's freshwater have only recently been identified as important repositories of organic matter (Lawson et al., 2014; Hood et al., 2015; Santibáñez et al., 2018) and biologically important nutrients (Bhatia et al., 2013; Hawkings et al., 2016; Wadham et al., 2016, Dubnick et al., 2017) that can be exported to marine environments. The

Greenland Ice Sheet is thought to dominate the fluxes from large ice sheets due to its high rate of glacier mass turnover via surface (supraglacial) melt and iceberg calving (Hood et al., 2015); however, the absence of data from the Antarctic ice sheet (AIS) has prevented meaningful comparison between the worlds' major ice sheets.

The beds of the Greenland Ice Sheet and AIS store large quantities of liquid water (e.g. Palmer et al., 2013; Siegert et al., 2016) in saturated sediments and sediment cavities. In Greenland, basal melt combined with supraglacial water that is directly transported to the bed (Das et al., 2008, Willis et al., 2015) cause subglacial "ponding" in areas where the ice is not frozen to the bed (Oswald et al., 2018). There are at least 400 subglacial lakes (Siegert et al., 2016) and extensive groundwater at the base of the AIS (Priscu et al., 2008) that are isolated from the surface by the ~1 to 4 km of ice. In contrast to the Greenland Ice Sheet, there is no evidence for the direct transfer of surface flow to the bed, with basal melt serving as the main source of subglacial water (i.e. Beem et al., 2010). The estimated volume of water (~10,000 km³) combined with biogeochemical data from the ice implies that these environments are significant global reservoirs of organic C (~1600 Tg C) and microorganisms (~10²¹ microbial cells) (Priscu et al., 2008).

Sedimentary basins beneath the AIS are estimated to store 21,000 petagrams of organic C (Wadham et al., 2012), making Antarctic subglacial environments potentially important contributors to global C budgets. However, quantification of Antarctic subglacial organic matter stores and their significance to regional biogeochemical processes is limited by a paucity of data and direct observations. Whillans Subglacial Lake (SLW) was the first Antarctic subglacial lake that was directly sampled using specialized clean access technology (Priscu et al., 2013) and characterized through physical, chemical, and microbiological investigations (Christner et al., 2014; Tulaczyk et al., 2014; Purcell et al., 2014; Achberger et al., 2016; Hodson et al., 2016; Michaud et al., 2016; Mikucki et al., 2016; Vick-Majors et al., 2016; Michaud et al., 2017). SLW is a relatively small body of fresh water (~0.13 km³; Christner et al., 2014; Fricker & Scambos 2009) located ~800 m beneath the West Antarctic Ice Sheet (Fricker et al., 2007). The geothermal heat flux into SLW exceeds the continental average (Fisher et al., 2015) and produces basal meltwater thought to release ice-entrained solutes, particulate matter, and atmospheric gases into the lake. Its water column and sediments were shown to contain diverse communities of bacteria and archaea that form a biogeochemically functional microbial ecosystem (Christner et al., 2014; Purcell et al., 2014; Achberger et al., 2016; Mikucki et al., 2016; Vick-Majors et al. 2016; Michaud et al., 2017). Because the thick ice cover isolates subglacial lakes from atmospheric exchange, solar radiation, and surface-derived melt water inputs, the chemical energy and nutrients required to support biological activity are derived from solutes, gases, minerals and particulate matter released from basal melting and those stored in the underlying sediments.

SLW is one of approximately 25% of Antarctic subglacial lakes that are considered hydrologically "active" (Smith et al., 2009), meaning that water movement occurs between lakes and to the coastal ocean via subglacial channels. Most of the active lakes are coastal (Fricker et al., 2007; Fricker & Scambos 2009), have fill-drain cycles of months to years (Siegfried & Fricker 2018), and discharge water under the grounded ice sheet into the sub-ice shelf ocean. There is also evidence for water flow from groundwater stored in East Antarctica (Foley et al.,

2019) and from lakes in the continental interior (Wright & Siegert 2012), implying wide hydrological dispersal of subglacial materials across Antarctica to the coastal margin.

West Antarctica's Gould-Siple Coast (hereafter referred to as "Siple Coast") is the location of one such active subglacial water system (Fricker et al., 2007), which drains fresh water through coastal estuaries into marine waters beneath the southern reaches of the Ross Ice Shelf (RIS) (Carter & Fricker 2012; Horgan et al., 2013; Muto et al., 2013). The outflows comprise a significant component of the overall freshwater budget of the coastal embayments, with episodic flow rates that can exceed $300 \text{ m}^3 \text{ s}^{-1}$ during major flooding events and generate variability in the RIS cavity freshwater budget (Carter & Fricker 2012). Such subglacial outflows have the potential to transport dissolved and particulate bioelements (e.g. C, N, P, Fe) stored on the Antarctic continent to the surrounding ocean (Statham et al., 2008; Wadham et al., 2013). These subglacially derived solutes and particulate matter could be of particular biogeochemical importance in Antarctica's coastal areas, 75% of which are covered by thick ice shelves (Rignot et al., 2013) that preclude photosynthetic primary production and effectively limit atmospheric inputs of solutes and particulate matter.

In this study we (i) characterize the organic matter and nutrient pools in SLW, (ii) determine the most likely sources of dissolved organic carbon to the lake water column, (iii) merge data from SLW with regional hydrological data (Carter & Fricker 2012) to estimate subglacial carbon and nutrient flows to the Siple Coast marine environment, and (iv) evaluate the potential geochemical and biological effects of this input to the dark marine coastal ecosystem beneath the RIS.

2 Methods

2.1 Site description

Whillans Subglacial Lake (SLW) lies beneath 800 m of ice on the Whillans Ice Stream (WIS; Christianson et al., 2012; Horgan et al., 2012). SLW receives basal melt water from the overlying ice sheet (Fisher et al., 2015) and upstream subglacial inflow (Carter & Fricker 2012; Horgan et al., 2013); its outflow drains to an embayment at the WIS grounding zone (GZ; sample location 84.3354 S, 163.6119 W) in the RIS cavity (Figure 1). The flow of water through SLW was characterized by analyzing ice surface changes using data derived from IceSat and surface GPS measurements (Siegfried et al., 2016), which revealed three fill and drain cycles between 2003 and 2015 (Siegfried et al., 2016). SLW was sampled in January 2013 when the lake was filling slowly after a drainage event in 2009 (Tulaczyk et al., 2014; Siegfried et al., 2016). The GZ site was 4.8 km downstream from the physical grounding line of the WIS (Figure 1). The ice cover at the GZ was ~760 m thick, and the underlying marine water column was ~10 m deep (Christianson et al., 2016; Begeman et al., 2018).

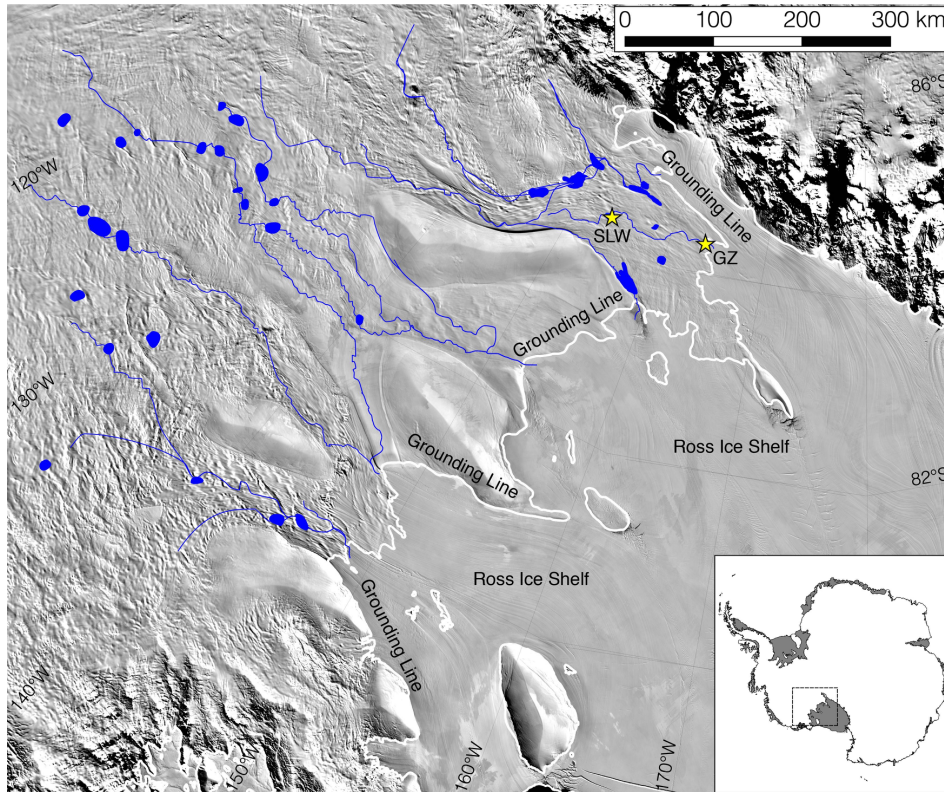


Figure 1. Map showing water flow paths from Siple Coast subglacial lakes to the RIS cavity. Blue lines = water flow paths, blue polygons = lakes, stars = subglacial access drilling sites: SLW = Whillans Subglacial Lake drill site, GZ = Grounding zone drill site. The grounding line is plotted in white. The study area is shown by the dashed box in the inset. The map was prepared using previously published data (Fricker et al., 2007; Smith et al., 2009; Fricker & Scambos 2009; Carter & Fricker 2012).

2.2 Sample collection

SLW water and sediments were collected through a ~0.6 m diameter borehole that was created with a microbiologically-clean, hot water drilling system (Priscu et al., 2013; Blythe et al., 2014; Burnett et al., 2014; Rack et al., 2014; Tulaczyk et al., 2014). Lake water samples were collected with a clean 10 L Niskin bottle and sediments were recovered using a clean gravity multicorer (Uwitec). Full details of the clean access protocol, results, drilling, and sample recovery are described elsewhere (Priscu et al., 2013; Christner et al., 2014; Tulaczyk et al., 2014; Achberger et al., 2016; 2017). Briefly, three discrete 10 L water samples were collected at mid-depth from the ~2.2 m water column between 28 and 30 January 2013 and returned to the surface for processing. Seawater at the GZ was collected from eight discrete 10 L Niskin casts between 9 January and 15 January 2015, using the same procedures described for SLW (Priscu et al., 2013; Tulaczyk et al., 2014). Samples were collected at sub-ice water column depths between 5 and 8 m in the 10 m water column.

For biological assays, sample water was decanted into acid-washed (0.1 M hydrochloric acid leached followed by 5 rinses with ultra-pure water) and autoclaved opaque high density polyethylene (HDPE) bottles. Acid-washed low density polyethylene (LDPE) bottles were used

for nutrients (Fe and dissolved N and P), and either acid-washed fluorinated HDPE bottles (Thermo Scientific, Nalgene, Waltham, MA) or acid-washed and combusted glass bottles were used for particulate and dissolved organic matter. Samples for Fe analysis were collected using trace-metal clean protocols following previously published methods (Turetta et al., 2004).

SLW sediment pore water samples were extracted at 2 cm intervals for analysis of dissolved organic matter using Rhizon pore water samplers (Rhizosphere; Seeberg-Elverfeldt et al., 2005) from a sediment core collected on 30 January 2013 (see Supplementary Table 1 for list of depths analyzed). The Rhizon samplers (0.2 μm filter pore size) were soaked in ultra-pure water before installation, and then inserted through pre-drilled holes in the sediment core liner. A 10 mL syringe was attached to the outlet, and the plunger was pulled and locked to maintain vacuum. After 14 h of extraction, the porewater was dispensed into 1M HCl washed, ultra-pure water rinsed (6X), and combusted (4 hr at 450 °C) glass vials. Procedural blanks consisting of ultra-pure water were analyzed in parallel and used to correct for solute introduced by the Rhizon samplers.

2.3 Organic matter and nutrients

Samples for DOC concentration and three-dimensional spectrofluorometric characterization of dissolved organic matter (excitation-emission matrix spectroscopy; EEMS) in the SLW water column were filtered through acid-leached and combusted (>4 h at 450 °C) 25 mm glass fiber filters (GF/F, effective retention size >0.7 μm). Filters were retained for particulate organic carbon (PC) and nitrogen analyses (PN) (Christner et al., 2014). The filtrate was collected in acid washed and combusted (>4 h at 450 °C) 40 mL amber borosilicate glass bottles fitted with polytetrafluoroethylene (PTFE) lined caps and stored at 4 °C until analysis at McMurdo Station (DOC) or upon return to Montana State University (EEMS). DOC and total dissolved N (TDN) concentrations were determined in water column and sediment porewater samples using a Shimadzu TOC-V Series TOC analyzer following acidification with hydrochloric acid to $\text{pH} \leq 2$ to remove inorganic carbon as CO_2 . Dissolved organic nitrogen (DON) was determined by subtracting DIN ($\text{DIN} = \text{NH}_4^+ + \text{NO}_2^- + \text{NO}_3^-$) from TDN. SLW water column DIN is from Christner et al., (2014); sediment porewater NH_4^+ was determined spectrophotometrically according to Strickland & Parsons (1968) and NO_3^- was determined via ion chromatography as described by Michaud et al., (2017).

Total dissolved and particulate phosphorus (TDP and PP, respectively) were determined spectrophotometrically (Solórzano & Sharp 1980) on water column samples partitioned by GF/F filtration as described above. Soluble reactive phosphorus values (approximate PO_4^{3-} from Christner et al., 2014) were subtracted from TDP to approximate dissolved organic phosphorus (DOP) for SLW. Sediment porewater PO_4^{3-} was determined via ion chromatography as described by Michaud et al., (2017).

EEMs were captured with a Horiba Jobin Yvon Fluoromax-4 Spectrophotometer (Horiba, Ltd., Japan) equipped with a Xe light source and a 1 cm path length quartz cuvette. Excitation wavelengths were measured every 10 nm from 240 nm to 450 nm, and emission wavelengths every 2 nm from 300 nm to 560 nm. Measurements were corrected for background (0.2 μm filtered ultra-pure water), Raman scattering, and inner-filter effects using absorbance spectra collected between 190 nm and 1100 nm with a Genesys 10 Series Spectrophotometer (Thermo

Scientific) (McKnight et al., 2001). Parallel factor analysis (PARAFAC) was used to decompose the trilinear EEMS arrays (Stedmon et al., 2003) and derive a four-component model that described the fluorescence characteristics of the pore water DOM using the drEEM toolbox (version 0.2.0) for Matlab (Murphy et al., 2013; see Supplemental Information and Supplemental Figures 1 - 3 for further details). The fluorescence intensity at the maximum for each component (F_{\max}) was calculated with drEEM by multiplying the maximum excitation loading and maximum emission loading for each component by its score. This approach produces intensities in the same measurement scale as the original EEMS and allows comparisons of maximum fluorescence between samples (Murphy et al., 2013). As an indicator of the relative contribution of fluorophores associated with labile organic moieties, the Freshness Index (FI) was determined at the excitation wavelength of 310 nm and by dividing the emission intensity at 380 nm (less decomposed DOM) by the maximum emission intensity between 420 nm and 436 nm (more decomposed DOM) by the (Parlanti et al., 2000; Huguet et al., 2009; Wilson & Xenopoulos 2009).

The stable isotopic compositions of water column particulate organic carbon and nitrogen ($\delta^{13}\text{C}$ and $\delta^{15}\text{N}$) were determined on acid-fumed samples (collected as described above) at the University of Washington IsoLab using a Costech elemental analyzer coupled to a MAT253 isotope ratio mass spectrometer with a Conflo III interface. Sediment samples were stored frozen, acid-fumed over 12M HCl, dried for 24 h at 90°C, and homogenized before analysis ($\delta^{13}\text{C}$ only) at the National Ocean Science Accelerator Mass Spectrometry (NOSAMS) facility. Samples were blank corrected and the isotope ratios are presented as per-mil deviations relative to Vienna Pee Dee Belemnite ($\delta^{13}\text{C}$) or Air-N₂ ($\delta^{15}\text{N}$) using standard delta notation.

Concentrations of Fe were determined on SLW water column samples that were filtered through 0.2 μm pore size filters (single-use syringe filter with PTFE membrane 0.20 μm , Sartorius Stedim Biotech GmbH, Göttingen, Germany) and then acidified with HNO₃ (Romil LTD – UPA grade) for >24 hours (dissolved Fe, including colloidal material). Unfiltered samples that were acidified with HNO₃ for >24 hours (total Fe) were also prepared. The samples were prepared in an Ultra-Clean Chemical Laboratory (UCCL) at the University of Venice and were analyzed 24 hours later using an ICP-SFMS (Inductively Coupled Plasma Sector Field Mass Spectrometry - Element2, Thermo Scientific, Bremen, Germany) coupled with a desolvation unit (Aridus, Cetac Technologies, Omaha, NE, USA). The instrument was housed in a dedicated laboratory with the sample introduction area protected by a laminar flow cabinet (Turetta et al., 2004). The quantification of Fe was carried out by a matched calibration method (Turetta et al., 2004). A multi-element standard solution (0, 10, 50, 100, 200, 500, 800, 1000, 2500 pg mL^{-1} , from a 10 mg L^{-1} ICP-MS calibration standard IMS102-Ultra Scientific (www.ultrasci.com) was added to nine aliquots of lake water sample. The accuracy of the measurements was determined using a certified reference material (TM-RAIN95). Particulate Fe was derived by subtracting the dissolved Fe from the total (unfiltered) Fe.

Fluxes of carbon and nutrients from the pore waters to the water column were calculated from 1 cm below the surface of the sediments to the bottom of the water column (0 cm sediment depth) assuming a well-mixed water column. The diffusion coefficient for DOC was the average diffusion coefficient determined over a range of DOC molecular weights (16 – 200,000) at 3 °C (Burdige et al., 1992) and was also used for DON. Diffusion coefficients associated with the lowest reported temperatures were used for NO₃⁻, NH₄⁺, and PO₄³⁻ (Li & Gregory 1974).

Diffusion coefficients were corrected for tortuosity (Shen & Chen 2007) and used a sediment porosity of 0.59 (based on a sediment depth of 0 to 2 cm).

2.4 Heterotrophic biomass production

Heterotrophic carbon production in the GZ water column was determined via [³H]L-leucine incorporation into acid-and-ethanol-insoluble macromolecules (Kirchman et al., 1985) in the same manner as for SLW (Christner et al., 2014). Samples (1.5 mL; three live and three 5% final v/v trichloroacetic acid [TCA] killed) were incubated with 20 nM radio-labeled leucine (specific activity 84 Ci mmol⁻¹) at 3 °C in the dark for 24 to 117 h. Separate experiments (Supplementary Figure 4) showed linear incorporation over this time period. Incubations were terminated by the addition of 100% cold TCA (5% v/v final TCA). Following centrifugation, the residual pellet was washed with cold (4 °C) 5% TCA and cold (4 °C) 80% ethanol, and then dried overnight at ~22 °C. One mL of Cytoscient ES scintillation cocktail was added to each vial and the radioactivity was quantified with a calibrated scintillation counter. Leucine incorporation rates (nM Leu d⁻¹) at the incubation temperature were converted to rates at in situ temperature (-1.9 °C) using an energy of activation of 25,755 J mol⁻¹, which was determined in separate experiments at SLW (Vick-Majors et al., 2016). Temperature corrected rates were converted to heterotrophic bacterial biomass production using published conversion factors of 1.42 x 10¹⁷ cells mol⁻¹ leucine (Chin-Leo & Kirchman 1988) and a cellular carbon content of 11 fg C cell⁻¹ (Kepner et al., 1998). The rate of heterotrophic bacterial carbon demand in SLW was determined as the sum of heterotrophic bacterial respiration (1.7 nmol C L⁻¹ d⁻¹) and incorporation of carbon (0.2 nmol C L⁻¹ d⁻¹) reported by Christner et al., (2014) and Vick-Majors et al., (2016).

The heterotrophic bacterial demand for C at the GZ was determined by summing the rates of carbon production described above with an estimated rate of bacterial carbon respiration. Carbon respiration was estimated by assuming a heterotrophic bacterial growth efficiency of 20% (average value determined from experiments in the Ross Sea; Carlson et al., 1999). N, P and Fe demand under the RIS at the GZ were calculated from rates of heterotrophic biomass production for carbon assuming Redfield stoichiometry (Redfield et al., 1963) and iron use in chemoorganotrophic growth (106:16:1:0.224; C:N:P:Fe, Raven 1988).

2.5 SLW carbon balance

The carbon balance for SLW was determined assuming steady state with respect to water:

$$\frac{dH_2O}{dt} = 0 \quad \text{Eq. 1}$$

where:

$$\frac{dH_2O}{dt} = I_{inflow} + I_{icemelt} - I_{outflow} \quad \text{Eq. 2}$$

I_{inflow} is equal to the rate at which water entered the lake during the preceding fill cycle (0.007 km³ a⁻¹, Siegfried et al., 2016) and $I_{icemelt}$ is described as:

$$I_{icemelt} = MR_{ice} * A_{SLW} \quad \text{Eq. 3}$$

where A_{SLW} is the previously determined lake surface area ($\sim 59 \text{ km}^2$; Fricker & Scambos 2009) and MR_{ice} (rate of ice melt over the lake) was determined previously (Fisher et al., 2015) and corrected for the relationship between the volume of ice and the volume of water contained in the ice ($V_{water} = 0.918 * V_{ice}$).

The annual change in water column DOC was calculated as:

$$\frac{dDOC}{dt} = J_{inflow} + J_{icemelt} + J_{sed} + J_{prod} - J_{BCD} - J_{outflow} \quad \text{Eq. 4}$$

where J_{inflow} , $J_{icemelt}$, J_{sed} , and J_{prod} are sources and J_{BCD} and $J_{outflow}$ are sinks and,

$$J_{inflow} = I_{inflow} * [DOC] \quad \text{Eq. 5}$$

where $[DOC]$ is $C_{DOClake}$ set to 50% of SLW $[DOC]$ and bounded by 100% of SLW $[DOC]$ (Christner et al., 2014) and the average $[DOC]$ of AIS ice (C_{DOCice} ; Hood et al., 2015),

$$J_{icemelt} = I_{icemelt} * C_{DOCice} \quad \text{Eq. 6}$$

$$J_{sed} = A_{SLW} * F_{DOCsed} \quad \text{Eq. 7}$$

where F_{DOCsed} (flux of DOC from the sediment porewaters) is calculated as described in section 2.3),

$$J_{prod} = V_{SLW} * R_{DOCprod} \quad \text{Eq. 8}$$

where $R_{DOCprod}$ is the volumetric rate of chemoautotrophic organic carbon production determined previously (Christner et al., 2014),

$$J_{BCD} = V_{SLW} * R_{DOCdem} \quad \text{Eq. 9}$$

where the volumetric heterotrophic bacterial organic carbon demand (R_{DOCdem}) was determined previously as the sum of organic carbon incorporated into biomass and respired to CO_2 (Vick-Majors et al., 2016),

$$J_{outflow} = I_{outflow} * C_{DOClake} \quad \text{Eq. 10}$$

The DOC accumulation time ($T_{DOClake}$) for the lake water column was determined as,

$$T_{DOClake} = \frac{C_{DOClake}}{dDOC/dt} \quad \text{Eq. 11}$$

The uncertainty in $T_{DOClake}$ calculations was estimated as follows: for parameters published elsewhere, the published uncertainty was used, for R_{DOCdem} and $R_{DOCprod}$, the propagated standard deviations of 3 replicate experiments were used; for C_{DOCice} , the range of values reported for AIS DOC concentrations (Hood et al., 2015) was used; for J_{inflow} , the concentration of DOC in the inflowing water was varied between that of SLW at the time of

sampling (221 μM) and the average concentration of C_{DOCice} ; sediment pore water to water column fluxes (F_{DOCsed}) were varied based on the range of possible DOC diffusion coefficients (Burdige et al., 2012). The upper bound for the annual DOC surplus was determined by subtracting the lowest J_{BCD} and J_{outflow} from the highest summed sources and the lower bound for the annual surplus was determined by subtracting the highest J_{BCD} and J_{outflow} from the lowest summed sources. All definitions are also provided with the mass balance in Table 2.

2.6 Bioelement export to the RIS cavity

To estimate the potential subsidies of organic carbon and inorganic nutrients (N, P, and Fe) from the Siple Coast to the sub-RIS cavity, the concentration of each bioelement in SLW water was multiplied by the volumetric flow rate of water from the Siple Coast to the sub-RIS cavity (0.82 to 15.8 $\text{km}^3 \text{a}^{-1}$, average, 1.9 $\text{km}^3 \text{a}^{-1}$; Carter & Fricker 2012). The impacts of subglacial flows of continental organic C and nutrients are likely greatest in coastal embayments (Carter & Fricker 2012), rather than being diluted into the entire volume of the RIS cavity ($\sim 125,000 \text{ km}^3$; Smethie & Jacobs 2005). The volume of the GZ embayments is not well constrained, but water column thickness is typically $< 50 \text{ m}$, and the embayment that receives outflow from SLW is $\sim 500 \text{ km}^2$ in area (Carter & Fricker 2012; Muto et al., 2013). Assuming a water column thickness of 50 m, an embayment volume of 25 km^3 was used for the calculations. There are six embayments associated with ice stream outflows along the Siple Coast (Carter & Fricker 2012), which if similar in volume, would total 150 km^3 . The contribution of organic C and nutrients per unit volume of water was calculated for coastal embayments under the RIS (150 km^3) as well as the contribution if diluted into the entire volume of the RIS cavity by dividing the total moles of each bioelement in the outflow on an annual basis by volume. To determine the potential biological subsidy from subglacial outflow, we compared the embayment contribution estimates to bacterial demand for organic C and nutrients at the GZ (section 2.4).

3 Results and discussion

Table 1. Dissolved and particulate matter concentrations (standard deviation) and bulk molar quantity or “pool size” in the SLW water column.

Parameter	DOC*	PC*	DON	PN*	DIN*	DOP	PP	SRP*	DFe	PFe	$\delta^{13}\text{C}$	$\delta^{15}\text{N}$
Concentration [†]	221 (55)	78.5 (7.4)	2.35 (0.80)	1.20 (0.40)	3.29 (0.79)	6.07 (0.63)	1.54 (0.57)	3.10 (0.70)	0.03 (0.02)	1.40 (0.44)	-26.2 (0.8)	9.9 -
Pool Size ($\times 10^5$ moles)	290	100	3.2	1.6	4.4	8.1	2.0	4.1	0.04	1.9	-	-

DOC, dissolved organic carbon; PC, particulate organic carbon; DON, dissolved organic nitrogen; PN, particulate nitrogen; DIN, dissolved inorganic nitrogen; DOP, dissolved organic phosphorus (difference between TDP and SRP); PP, particulate phosphorus; SRP, soluble reactive phosphorus (\sim dissolved inorganic P); DFe, dissolved Fe; PFe, particulate Fe. DOC, PC, DON, PN, DIN, SRP n = 3; TDP n = 5; PP n = 4; $\delta^{15}\text{N}$ -PN n = 1; $\delta^{13}\text{C}$ -PC n = 2.

* reported in Christner et al., 2014.

[†] Concentrations are given in $\mu\text{mol L}^{-1}$; $\delta^{13}\text{C}$ and $\delta^{15}\text{N}$ values are in ‰

The primary source of SLW water is glacial meltwater from the West Antarctic Ice Sheet, with a minor contribution (~6%) from relict seawater in the deepest sediment pore waters (Christner et al., 2014; Michaud et al., 2016). Information on carbon and nutrient concentrations from polar ice sheets are limited, but available data show low concentrations relative to many temperate systems ($\text{DOC} \sim 12.5 \mu\text{mol C L}^{-1}$, Hood et al., 2015; $\text{NH}_4^+ \sim 0.05 \mu\text{mol N L}^{-1}$, $\text{NO}_3^- \sim 0.6 \mu\text{mol N L}^{-1}$, Wolff 2013; $\text{PO}_4^{3-} \sim 0.2 \mu\text{mol P L}^{-1}$ for the Greenland ice sheet, Kjær et al., 2011, no P data are available from the Antarctic ice sheet). By contrast, the SLW water column had relatively high concentrations of organic matter and inorganic nutrients (Table 1, Figure 2, Christner et al., 2014), suggesting sedimentary sources and/or production in situ.

3.1 Organic matter and inorganic nutrients in the SLW water column and sediments

The PC concentration in the SLW water column was $78.5 \mu\text{mol C L}^{-1}$ (Christner et al., 2014). Given the microbial cell density in the lake water (1.3×10^{-8} cells L^{-1} , Christner et al., 2014), and a cellular carbon content estimate of $0.9 \text{ fmol C cell}^{-1}$ (Kepner et al., 1998), only $\sim 0.1 \mu\text{mol PC L}^{-1}$ could be associated with intact microbial biomass. This indicates that most of the water column PC was detrital. Suspended particulate organic matter (POM) was N-poor relative to C and P (65 C:N; 0.78 N:P by atoms), compared to atomic elemental ratios for freshwater bacteria in a range of lakes (C:N = 7.3; N:P = 12; Cotner et al., 2010). The sediment C:N ratio, while lower than that of the water column was, on average, still a factor of 2 greater than that of that previously reported for freshwater bacteria (SLW sediment C:N average = 15 ± 1.2 ; Figure 2; PC and PN composition of sediment samples from 0 – 37 cm was reported previously [Christner et al., 2014; Michaud et al., 2017] and the profile is shown in the results of this paper for ease of interpretation). The highest sediment PC:PN occurred in the top 2 cm of the sediment profile (PC:PN = 18) and may be explained by microbial utilization of POM targeting N-rich compounds. A similar pattern was observed in the DOM pool in the SLW water column, where the atomic C:N ratio of DOM (95) exceeded that of freshwater bacteria by a factor of 13. In contrast, the average for the sediment pore waters exceeded the C:N ratio of freshwater bacteria by only a factor of ~ 3.5 . (atomic DOM ratio = 18 C:N).

393 The DOM pool in the water column was also N-poor relative to P (DON:DOP =
394 0.38). The composition of the total dissolved N pool in the water column and sediment pore
395 waters were similar, with DON accounting for 40% of water column total dissolved N (TDN)
396 and 39% of average sediment pore water TDN. In both cases, the dissolved inorganic N (DIN)
397 pool was dominated by NH_4^+ (73% in the water column, Christner et al., 2014; 86% in the
398 sediment pore waters on average, Figure 2). While runoff from the surrounding watershed and
399 direct atmospheric deposition are primary sources of DON in temperate freshwater environments
400 (Berman & Bronk 2003), SLW's thick ice cover and relative isolation from exposed land surface
401 and the low N concentrations in glacial ice (Wolff 2013) make these sources less likely to be of
402 importance. Biological production, which is the major source in open-ocean waters far from
403 terrestrial inputs (Berman & Bronk 2003) and DON released from the sediments, which is
404 common in shallow, freshwater environments (Zehr et al., 1988), are likely sources. Based on
405 PC:PN ratios, the SLW surface sediments and pore waters were rich in PON relative to the water
406 column (Figure 2). Porewater DON concentrations peaked in the surficial sediments, indicating
407 the pore waters were a source of DON to the water column. However, DON concentrations
408 decreased with depth along the sediment pore water profile, and thus, are not consistent with a
409 source of DON from relict organic matter or bedrock N at depth. These data imply that
410 contemporary biological activity in the surface sediments (0 to 2 cm) is likely the primary source
411 of DON in SLW. The thick ice-cover that overlies SLW precludes photochemical decomposition
412 of DON, which is an additional sink in open water environments and often results in the
413 production of DIN (e.g. Vähätalo & Zepp 2005; Porcal et al., 2014). Thus, darkness in the
414 subglacial environment may contribute to an accumulation of recalcitrant DON and tight cycling
415 of labile DON (e.g. urea, amino acids).

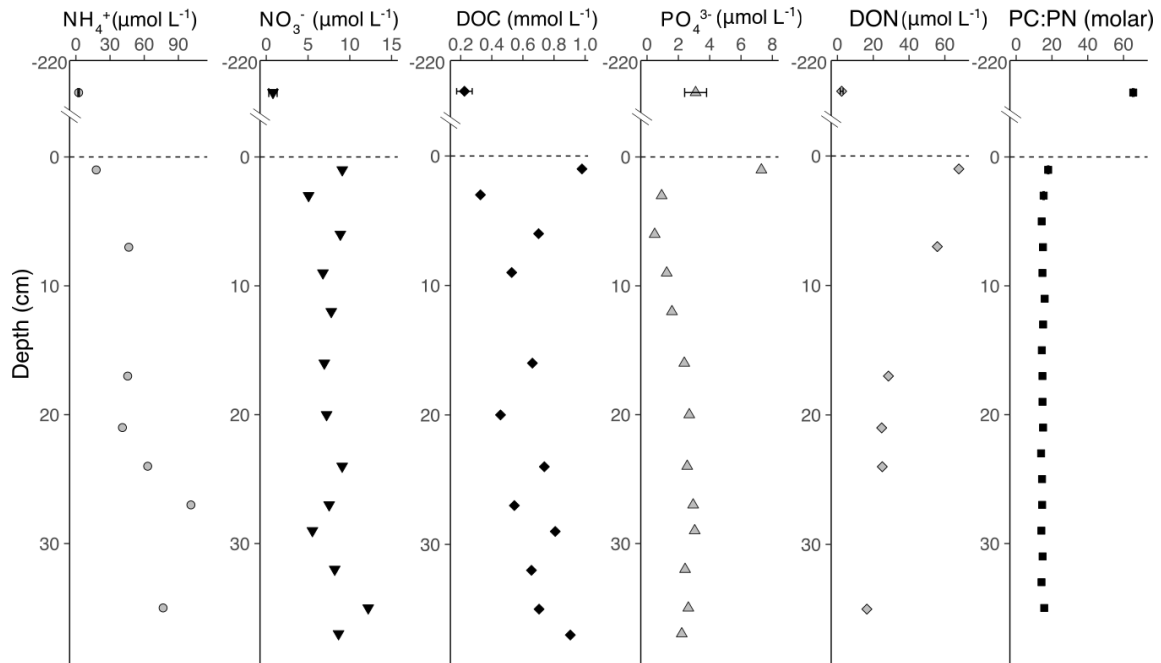


Figure 2. SLW water column and sediment porewater chemical profiles inorganic N, P, dissolved organic matter (DOC, DON), and PC:PN ratios. Note that PO_4^{3-} was measured as soluble reactive phosphorus (SRP) in the water column and in ion form in the sediment porewaters. The dashed line indicates the sediment-water interface. Water column samples were collected from the middle of the 2.2 m deep water column. Water column values for DOC, NH_4^+ , NO_3^- , and SRP and sediment C:N were published previously (Christner et al., 2014, Michaud et al., 2017). Note the difference in units for DOC. Sediment pore water sample depths are in Supplementary Table 1.

3.2 Biogeochemical characteristics of particulate and dissolved organic matter in SLW

The $\delta^{13}\text{C}$ of PC from three sediment depths (0-2 cm, top; 20-22 cm, middle; and 32-34 cm, bottom) and from suspended material in the water column was determined to further characterize the organic matter in SLW. There was little variation in $\delta^{13}\text{C}$ -PC among sediment depths (average = $-25.2 \text{ ‰} \pm 0.3$). The sediment and water column $\delta^{13}\text{C}$ -PC (water column average = -26.2 ‰ , range = -25.6 to -26.8 ‰ ; $n=2$) were also similar. This similarity in $\delta^{13}\text{C}$ -PC between the water column and sediments, coupled with the 4-fold increase in PC:PN ratio between the sediments and water column (water = 65.4, surface sediments = 17.9), and high $\delta^{15}\text{N}$ value of PN (9.9 ‰) in the water column further supports that the lake water contains relict detritus from which N has been scavenged to support biological activity. The $\delta^{13}\text{C}$ and C:N ratios of SLW sediments closely align with pre-Last Glacial Maximum sediments collected from former Subglacial Lake Hodgson ($\delta^{13}\text{C} \sim -25$, C:N ~ 10 -15), a recently-exposed subglacial lake on the Antarctic Peninsula (Hodgson et al., 2009). The $\delta^{13}\text{C}$ is similar to the $\delta^{13}\text{C}$ for the deep pelagic waters of stratified, permanently ice-covered lakes in the Taylor Valley of East Antarctica ($\leq -26 \text{ ‰}$; Lawson et al., 2004). These lakes are characterized by strong chemoclines, with carbon cycling below the chemoclines heavily influenced by relict organic matter.

The DOC concentration in SLW ($221 \mu\text{mol C L}^{-1}$, Table 1; Christner et al., 2014) was an order of magnitude higher than an average compiled for Antarctic glacial ice determined based on a range of ice sheet and valley glacier sites ($12.5 \mu\text{mol L}^{-1}$; Hood et al., 2015), but similar to that of the water columns of other ice-covered Antarctic surface lakes ($\sim 200 \mu\text{mol L}^{-1}$; Takacs et al., 2001), and of the same order of magnitude as more concentrated subglacial groundwater systems ($420 \mu\text{mol L}^{-1}$; Mikucki et al., 2009). Concentrations were also similar to maximum estimates for the water column of Vostok Subglacial Lake, which indicated an advected or internal biological source of DOC to the lake ($250 \mu\text{mol L}^{-1}$; Priscu et al., 1999, Christner et al., 2006). Given that glacial meltwater that is less concentrated in carbon and nutrients comprises the major water source to SLW (Christner et al., 2014; Michaud et al., 2016), we examined the composition and sources of DOM using fluorescence spectroscopy to describe the composition of the SLW DOM pool and used a mass-balance approach to quantify sources of organic C to the water column.

3.3 Fluorescence characterization of water column and sediment porewater DOM

A fraction of DOM is fluorescent (FDOM) and its fluorescence excitation and emission properties provide signatures of its chemical composition and sources (Romera-Castillo et al., 2011). Parallel factor analysis (PARAFAC) of excitation/emission fluorescence of FDOM in SLW sediment porewaters (Figure 3 and Supplementary Figure 1) was used to characterize the FDOM in SLW. Our analysis revealed the presence of four fluorophore components (C1-C4) (Supplementary Figure 2), including two that were amino acid-like (tyrosine-like and tryptophan-like, C3 and C4, respectively) and indicative of microbial DOM production. C3 and C4 accounted for $\sim 70\%$ of total FDOM in the surface porewaters (0-2 cm), and decreased to $\sim 50\%$ at depths of 36-38 cm, while humic-like fluorophores (C1 and C2) increased in relative abundance within the deeper sediments (Figure 3). C3 was the dominant component in the top 15 cm of the porewater profile, accounting for between 31.9% and 41.6% of the FDOM. This depth range is consistent with the oxygen penetration depth in the SLW sediments (inferred from the profile of redox-sensitive vanadium in the sediment porewaters), which suggests oxygen-consuming microbial activity occurs in the top 15 cm of sediment (Michaud et al., 2016). Because the FI is thought to be related the degree of organic matter degradation or lability (Parlanti et al., 2000; Wilson & Xenopoulos 2009), we examined the FI (Figure 3) with this potential zone of microbial activity in mind.

The FI showed little variation with depth in the sediment porewaters after decreasing from 1.28 to 1.11 between the water column and top 2 cm of sediment (sediment porewater slope = -0.0008 ; Figure 3). None of the fluorophore components had strong explanatory power over FI in the sediment porewater profile (C1, C2, C3, C4: $R^2 = 0.07, 0.001, 0.23$, and 0.07 , respectively; slope = $0.0020, 0.0003, -0.0026$, and 0.0020 FI units $[\text{component } \%]^{-1}$, respectively). C3 explained the greatest amount of variation in FI, and was the only component negatively correlated with FI (albeit with marginal statistical significance; $R^2 = 0.23$, slope = -0.0026 , $P = 0.1$). If the FI is indeed related to the degree of organic matter degradation in this system, where higher FI is analogous to greater contributions from less degraded OM, the inverse relationship between C3 and FI could indicate that C3 is a product of the microbial degradation of organic

matter. That the relative contribution of C3 decreased with depth also suggests that it may be related to microbial activity.

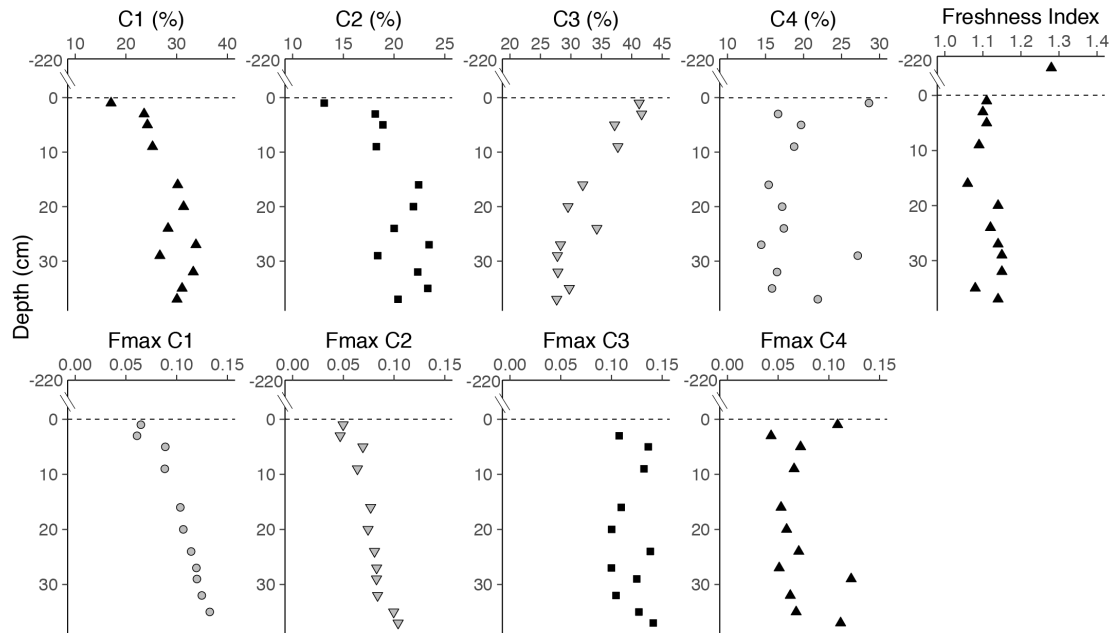


Figure 3. Fluorescence characteristics of SLW sediment pore water DOM. Components C1 and C2 (humic-like) and C3 and C4 (protein-like) shown as % of total fluorescence. F_{\max} = maximum fluorescence calculated as described in the methods. The Freshness Index was calculated for sediment pore waters and the water column, as described in the methods.

While the contributions from C3 and C4 did decrease with depth, the increase in humic-like fluorescence at depth was not simply a result of decreasing fluorescence in the non-humic-like components, as demonstrated by the maximum fluorescence intensity for each component (F_{\max}) through the pore water profile (Figure 3). The F_{\max} for humic components C1 and C2 increased linearly with depth (slope = 0.002 fluorescence units cm^{-1} , $R^2 = 0.9$ and slope = 0.001 fluorescence units cm^{-1} , $R^2 = 0.9$, respectively), while the F_{\max} for amino-acid like components C3 and C4 remained constant (slope = -0.003 fluorescence units cm^{-1} , $R^2 = 0.05$ and slope = 0.0004 fluorescence units cm^{-1} , $R^2 = 0.04$, respectively; Figure 3). The combination of increased humic-like fluorescence and increasing DOC concentration at depth (slope = 0.03 $\mu\text{M cm}^{-1}$, $R^2 = 0.22$) suggests that greater proportions of less labile and/or more heavily modified FDOM are stored deeper in the sediments.

In contrast to the four components identified from the sediment pore waters, a fluorescent DOM peak with modified tyrosine-like fluorescence was identified in the water column, (ex: 240 nm: 310 nm; Supplementary Figure 3). The single identifiable water column peak was blue-shifted from the tyrosine-like C3 observed in the pore waters (ex: 270 nm: 300 nm; Supplementary Figure 2). The peak was also similar to a fluorophore identified in ice samples from the West Antarctic Ice Sheet Divide ice core (D'Andrilli et al., 2017). A blue shift may indicate a decrease in aromaticity or molecular mass resulting from biological activity (Coble 1996). Together with the above analysis indicating that C3 may be associated with microbial activity, these results suggest

that the water column FDOM composition is influenced by water source and microbial processing and of porewater DOM.

We compared our PARAFAC model results to published literature and other models in the OpenFluor database (Murphy et al., 2014). The humic-like C2 identified in SLW matched components from other models in the OpenFluor database (95% similarity cutoff): component that was produced along a river-to-marine transition in an Arctic river delta in Siberia (Gonçalves-Araujo et al., 2015), a component that was linked to microbial degradation of FDOM in five large Arctic rivers (Walker et al., 2013), and a component from Belgian rivers, which was also linked to microbial activity (Lambert et al., 2017). SLW's C2 was similar, in terms of its excitation/emission maxima, to the mixture of humic peaks commonly associated with coastal environments (Coble 1996), and microbial degradation and production of DOM in Antarctic surface lakes (Cory & McKnight 2005). The C1 humic-like fluorophore did not match components in the OpenFluor database, but was similar to a microbially-derived component from a permanently ice-covered McMurdo Dry Valley lake (Cory & McKnight 2005), a typical marine humic component (Coble 1996), and DOM associated with microbial degradation of organic matter in Antarctic mountain glaciers (Barker et al., 2010). While presumed to be biologically recalcitrant, some humic components can also be consumed by microorganisms (Romera-Castillo et al., 2011), implying that the humic-like FDOM detected in SLW porewaters may be a biologically useful energy source. Since FDOM in glacier ice is typically dominated by protein-like fluorescence (e.g. Dubnick et al., 2010), the humic-like fluorescence in the porewaters is more likely a signature of microbial activity than of the ice-melt source-waters and the similarities between SLW humic components and those matched in OpenFluor imply a common component of DOM from microbial activity in ecological settings that share characteristics with SLW (i.e., cold and dark with microbially dominated biogeochemical processes).

3.4 Sources of dissolved organic matter and nutrients to the SLW water column

The estimated residence time of glacial till pore water beneath the Whillans Ice Stream (1000 - 10,000 a) implies that subglacial water in the region should be rich in accumulated solutes (Christoffersen et al., 2014). In contrast, the bulk residence time for the water column in SLW is much shorter (years to decades) (Fricker et al., 2007; Siegfried et al., 2014). Consequently, the solute pool in SLW likely results from a mixture of shorter-term lake-basin and longer term till-porewater processes (Michaud et al., 2016). We calculated diffusive fluxes from sediment pore waters to the water column for DOC, DON, SRP (PO_4^{3-}), NO_3^- -N, and NH_4^+ -N. The highest contributions of biologically relevant solutes from the sediment pore waters were for DOC and DON at 5.6×10^6 and $4.8 \times 10^5 \text{ mol a}^{-1}$, respectively. The inorganic nutrients, NH_4^+ , NO_3^- , and PO_4^{3-} , had significantly lower contributions from the sediments (0.82, 0.10, and 0.16 mol a^{-1} , respectively).

The SLW FDOM data revealed that organic matter in the subglacial waters was derived from and/or altered by microbial activity; however, contemporary microbial activity alone cannot account for the size of the observed DOC pool (Table 2). In addition to chemoautotrophic C-fixation (Christner et al., 2014) and flux from the sediment porewaters, sources of DOC to the SLW water column include water inflow from upstream to the lake and ice melt above the lake, with the total input from all sources estimated at 6.4×10^6 mol C a⁻¹ (Table 2). DOC input to the water column was dominated by DOC flux from the sediment pore waters (86% of total DOC inputs) followed by estimated inflow from upstream (12%), chemoautotrophic production (2.0%) and ice melt over the lake basin (0.2%).

Heterotrophic bacterial carbon demand (T_{DOCdem}) is the major biological DOC sink in SLW. The DOC supply estimated by our model exceeds this metabolic sink by a factor of 70. Therefore, most of the DOC input to the SLW water column accrues to the DOC pool (Table 2). These calculations yield an accumulation time of 6.3 years (range = 4.8 – 11.9) (Table 2), a timeframe similar to the variable fill-drain cycles of lakes in this region (Siegfried et al., 2014). These estimates highlight the importance of sediment pore water interactions and SLW watershed hydrological connectivity in accounting for the geochemical and biological processes occurring in the lake.

According to our calculations, sediment pore water DOM was the largest contributor to the water column DOC budget. However, the water column DOM fluorescence was dominated by a single amino-acid-like fluorophore characterized by a blue shift from the dominant porewater fluorophore, C3. The small number of water column samples ($n = 3$) precluded the use of PARAFAC analysis and may have diminished our ability to distinguish the presence of other fluorophores. The differences between water column and sediment porewater DOM character may be explained by the consumption of sediment-derived DOM in the water column or at the water-sediment interface. The DOC concentration decreased by a factor of 4.5 between the surface sediment pore waters and the water column, or taking the average of the top ten centimeters of the sediments, by a factor of 2.7, implying that sediment derived DOC was consumed in the water column or at the interface. At the same time, the F_{max} of the humic-like components, C1 and C2, decreased by 51% and 42%, respectively, in the surface sediments (0-2 cm) relative to the average for the rest of the sediment column (2-38 cm) (Figure 3). These results, together with the similarity between C1 and C2 and components that were produced and consumed by microorganisms in similar environments (Section 3.3), suggest that sediment-derived DOM is transformed by microbial activity in the water column and/or at the sediment-water interface, resulting in a water column dominated by microbially produced tyrosine-like FDOM.

Table 2. Parameters and values in the Subglacial Lake Whillans DOC mass balance

	Parameter	Symbol or derivation	Value (Range)	Units	References
Constants	Ice melt rate	MR_{ice}	1.7×10^{-5} ($1.2 \times 10^{-5} - 2.1 \times 10^{-5}$)	km liquid water a^{-1}	Fisher et al., 2015
	Lake surface area	A_{SLW}	59 (47 – 71)	km ²	Fricker & Scambos 2009
	Water column depth	D	0.0022	km	Christner et al., 2014
	Volume of SLW	$V_{SLW} = D \times A_{SLW}$	0.13 (0.10 – 0.16)	km ³	Christner et al., 2014, Fricker & Scambos 2009
	SLW [DOC]	$C_{DOC_{lake}}$	2.2×10^8 ($1.7 \times 10^8 - 2.8 \times 10^8$)	mol km ⁻³	Christner et al., 2014, Fricker & Scambos 2009
	Ice [DOC]	$C_{DOC_{ice}}$	1.3×10^7 ($1.7 \times 10^6 - 2.7 \times 10^7$)	mol km ⁻³	Hood et al., 2015
	Areal flux from sediments	$F_{DOC_{sed}}$	9.3×10^4 ($5.5 \times 10^4 - 1.3 \times 10^5$)	mol km ⁻² a ⁻¹	This paper
	Volumetric C production	$R_{DOC_{prod}}$	1.0×10^{-6} ($8.7 \times 10^{-7} - 1.1 \times 10^{-6}$)	mol km ⁻³ a ⁻¹	Christner et al., 2014
	Volumetric C demand	$R_{DOC_{dem}}$	6.7×10^{-7} ($5.3 \times 10^{-7} - 8.1 \times 10^{-7}$)	mol km ⁻³ a ⁻¹	Vick-Majors et al., 2016
Water	Water from ice melt	$I_{icemelt} = MR_{ice} \times A_{SLW}$	9.8×10^{-4} ($7.0 \times 10^{-4} - 1.3 \times 10^{-3}$)	km ³ a ⁻¹	Fisher et al., 2015, Fricker & Scambos 2009
	Water from inflow	I_{inflow}	7.0×10^{-3}	km ³ a ⁻¹	Siegfried et al., 2016
	Water outflow	$I_{outflow} = I_{icemelt} + I_{inflow}$	7.9×10^{-3} ($7.7 \times 10^{-3} - 8.3 \times 10^{-3}$)	km ³ a ⁻¹	This paper
DOC sources	Inflow	$J_{inflow} = C_{DOC_{lake}} \times I_{inflow}$	7.7×10^5 ($9.3 \times 10^4 - 1.9 \times 10^6$)	mol a ⁻¹	This paper
	Ice melt	$J_{icemelt} = I_{icemelt} \times C_{DOC_{ice}}$	1.2×10^4 ($1.7 \times 10^3 - 2.8 \times 10^4$)	mol a ⁻¹	This paper
	Sediment porewater	$J_{seds} = F_{DOC_{sed}} \times A_{SLW}$	5.6×10^6 ($3.3 \times 10^6 - 7.7 \times 10^6$)	mol a ⁻¹	This paper
	Chemoautotrophic production	$J_{prod} = R_{DOC_{prod}} \times V_{SLW}$	1.3×10^5 ($1.1 \times 10^5 - 1.5 \times 10^5$)	mol a ⁻¹	This paper
sinks	C demand	$J_{BCD} = R_{DOC_{dem}} \times V_{SLW}$	8.7×10^4 ($6.8 \times 10^4 - 1.0 \times 10^5$)	mol a ⁻¹	This paper
	DOC outflow	$J_{outflow} = I_{outflow} \times C_{DOC_{lake}}$	1.8×10^6 ($1.3 \times 10^6 - 2.3 \times 10^6$)	mol a ⁻¹	This paper
Balance	Surplus	$dDOC/dt = J_{inflow} + J_{icemelt} + J_{seds} + J_{prod} - J_{BCD} - J_{outflow}$	4.5×10^6 ($2.1 \times 10^6 - 7.4 \times 10^6$)	mol a ⁻¹	This paper
	Accumulation Time	$T_{DOC_{lake}} = C_{DOC_{lake}} / (dDOC/dt)$	6.3 (4.8 – 11.9)	a	This paper

3.5 Subglacial bioelement subsidies to the Siple Coast

The Ross Ice Shelf (RIS) covers ~500,000 km² of the Ross Sea (Rignot et al., 2013). At its southern extent, it adjoins the Siple Coast where the ice shelf flows north towards the open Ross Sea (Figure 1). Biogeochemical data on the waters from ~450 km from the edge of RIS were collected from under the RIS as part of the Ross Ice Shelf Project at Station J9 (Clough & Hansen 1979). The J9 sediment and water column studies showed microbial communities capable of metabolizing organic carbon substrates and fixing inorganic C in the dark (Horrigan

1981), and a benthic community dominated by scavengers (Lipps et al., 1979). Data from closer to the ice shelf margin (Vick-Majors et al., 2015) revealed dark inorganic C-fixation rates similar to those determined by Horrigan (1981; $\sim 6 \text{ nmol C L}^{-1} \text{ d}^{-1}$) that were exceeded by heterotrophic microbial carbon demand. These results imply that in situ carbon production is insufficient to sustain the carbon demand under the RIS and that other sources of DOC are required. DOC in the RIS cavity source waters (mixtures of High and Low Salinity Shelf Water produced in the Ross Sea) may supplement the reduced C source under the ice shelf. However, long residence times (~ 3.5 years; Smethie et al., 2005) provide time for drawdown of supplemental DOC under the ice during water mass transport. Indeed, DOC concentrations in source waters beneath (Vick-Majors et al., 2014) or proximate to (Bercovici et al., 2017) the McMurdo Ice Shelf were approximately $40 \text{ } \mu\text{mol C L}^{-1}$ ($\sim 37 \text{ } \mu\text{mol C L}^{-1}$, Vick-Majors et al., 2015; $\sim 47 \text{ } \mu\text{mol C L}^{-1}$ in Ross Sea Dense Shelf Water, Bercovici et al., 2017), while average DOC concentrations in water collected at the GZ were approximately twice these values ($75 \text{ } \mu\text{mol C L}^{-1}$). Apparent DOC enrichment at the GZ raises the possibility that subglacial outflows could be an important subsidy to coastal and estuarine biogeochemical processes under the RIS.

Subglacial water from the Siple Coast ice streams enters the RIS cavity (Figure 1) both continuously and in pulses during lake discharge events at rates of 0.82 to $15.8 \text{ km}^3 \text{ a}^{-1}$ (average, $1.9 \text{ km}^3 \text{ a}^{-1}$; Carter & Fricker 2012). Based on measured values of dissolved and particulate organic matter in SLW (Table 1; this study and Christner et al., 2014) and water discharge estimates (Carter & Fricker 2012; Table 3), the average input of total organic carbon to the RIS cavity is $5.7 \times 10^8 \text{ mols C y}^{-1}$. Average inputs of inorganic N and P are 100-fold lower, and dissolved Fe 10,000-fold lower (Table 3) than estimates for organic carbon. The organic carbon input to coastal waters is similar in magnitude to that at an Arctic glacier catchment in Greenland (average $2.8 \times 10^8 \text{ mols C a}^{-1}$; Lawson et al., 2014), where glacial runoff is an important source of organic C to the ocean (Hood et al., 2015).

To determine the potential for subglacial outflows to subsidize biological activity beneath the RIS, we estimated masses of organic C and inorganic N, P, and Fe required to support heterotrophic bacterial activity at the GZ. The heterotrophic bacterial demand for organic C and nutrients under the RIS based on rates of ^3H -leucine incorporation and estimated bacterial growth efficiency at the GZ was $0.19 \text{ nmol C L}^{-1} \text{ d}^{-1}$; (S.D. = 0.1; $n = 4$). Extrapolating this demand to the estimated volume of the Siple Coast embayments (150 km^3) yields an organic C demand of $1.0 \times 10^7 \text{ mols C a}^{-1}$; using the entire volume of water under the RIS ($125,000 \text{ km}^3$; Smethie et al., 2005) yields an organic C demand of $1.8 \times 10^9 \text{ mols C a}^{-1}$. Based on the Redfield ratio (106:16:1; C:N:P by atoms) extended to include the Fe demand for chemoorganotrophic growth (Raven 1988), the nutrient demands are one (N) to three (P and Fe) orders of magnitude lower than for carbon (Table 3).

Table 3. Bioelemental subglacial flows to the Ross Ice Shelf (RIS) cavity from the Siple Coast compared to estimated bacterial carbon and nutrient demand at the GZ.

<i>Element</i>	<i>Demand (moles a⁻¹)</i>	<i>Outflow (moles a⁻¹)</i>			<i>% of demand met by outflow</i>		
		<i>Avg</i>	<i>Min</i>	<i>Max</i>	<i>Avg</i>	<i>Min</i>	<i>Max</i>
Organic C	1.0 x 10 ⁷	5.7 x 10 ⁸	2.5 x 10 ⁸	4.7 x 10 ⁹	5400 (6.5)	2400 (2.8)	45000 (54)
DIN	1.6 x 10 ⁶	6.2 x 10 ⁶	2.7 x 10 ⁶	5.2 x 10 ⁷	390 (0.47)	170 (0.21)	3300 (4.0)
Org N		4.6 x 10 ⁶	3.3 x 10 ⁶	2.1 x 10 ⁷	290 (0.35)	210 (0.25)	1300 (1.6)
SRP	9.8 x 10 ⁴	5.9 x 10 ⁶	2.5 x 10 ⁶	4.9 x 10 ⁷	5900 (7.2)	2600 (3.1)	50000 (60)
Org P		9.0 x 10 ⁶	7.3 x 10 ⁶	3.0 x 10 ⁷	9200 (11)	7500 (8.9)	31000 (37)
dFe	2.2 x 10 ⁴	6.1 x 10 ⁴	2.6 x 10 ⁴	5.1 x 10 ⁵	280 (0.33)	120 (0.14)	2300 (2.8)
pFe		2.7 x 10 ⁶	1.2 x 10 ⁶	2.3 x 10 ⁷	12000 (15)	5400 (6.4)	100000 (120)

Demand = bacterial elemental demand in Siple Coast embayments. Embayment volume estimated as described in Methods. DIN = dissolved inorganic nitrogen. SRP = soluble reactive phosphorus. dFe = dissolved Fe, pFe = particulate Fe. Organic C, N, and P are the sum of dissolved and particulate fractions. % of demand met by subglacial outflow assumes a 150 km³ embayment size; value in parentheses assumes volume of the entire RIS cavity (125,000 km³).

Based on our estimates, organic C supplied to the GZ coastal embayments by subglacial outflows can support, on average, 5400% of heterotrophic microbial demand for organic C, 390% of inorganic N demand, and 5900% of inorganic P demand (Table 3). Subglacial outflow may also be a major source of particulate Fe (pFe; Table 3), although the bioavailability of the pFe remains uncharacterized. Together, these calculations show that subglacial outflow may be of particular importance to coastal marine ecosystems beneath the RIS, as the inferred affect is substantially reduced if well mixed with the entire volume of water under the RIS (Table 3). The calculated outflows are also greater sources of C and P than N, a conclusion that is consistent with those drawn from modelled estimates of nutrient outflows in meltwater from the Greenland (Lawson et al., 2014; Hawkings et al., 2016) and Antarctic (Wadham et al., 2013) ice sheets. Overall, our biogeochemical results and related calculations reveal that subglacial outflows may provide coastal microbial communities on the Siple-Gould Coast with C and P at rates sufficient to support marine biomass production.

4 Conclusions

Based on data from SLW, biologically-relevant solutes accumulate within subglacial waters during the decadal scale flushing time of the lake as a result of sediment pore water interactions, contemporary microbial activity, and the lack of a photochemical sink for organic matter. Microbial processing of DOM resulted in a downward sediment porewater to water column gradient in SLW DOC concentration with amino-acid-like fluorescence dominating the

biologically active sediment layers and the water column. Our results show that the subglacial DOM composition results not only from relict organic matter, but also from microbial activity under the West Antarctic Ice Sheet. The DOM and other solutes are likely to be released to the Siple Coast during subglacial drainage events at rates significant for fertilizing coastal marine communities in the expansive and dark RIS cavity. The effect of subglacial outflows on biogeochemical processes in coastal Antarctica should not be restricted to the Siple Coast because active subglacial lakes have been cataloged in other coastal regions of both East and West Antarctica (Siegfried & Fricker 2018). An estimated $52.8 \text{ km}^3 \text{ a}^{-1}$ of subglacial meltwater drains to the Southern Ocean from Antarctica (Wadham et al., 2013), and extrapolation of our solute flux data to this volume of water yields total subglacial drainage fluxes of $\sim 1.6 \times 10^{10} \text{ mol}$ of organic C a^{-1} associated with this subglacial drainage. This flux is similar to the predicted contributions from Antarctic surface runoff ($\sim 2 \times 10^{10} \text{ mol C a}^{-1}$, Hood et al., 2015; maximum $2.1 \times 10^{10} \text{ mol C a}^{-1}$; Wadham et al., 2013). Collectively, our results demonstrate that inputs of microbially-modified organic matter and nutrient flux from subglacial environments are of a significant magnitude to affect neritic, and perhaps pelagic, productivity in the Southern Ocean, and may be of particular relevance to ecosystem productivity beneath ice shelves that lack direct photoautotrophic inputs of organic matter.

Acknowledgments

The Whillans Ice Stream Subglacial Access Research Drilling (WISSARD) project was funded by National Science Foundation grants (0838933, 0838896, 0838941, 0839142, 0839059, 0838885, 0838855, 0838763, 0839107, 0838947, 0838854, 0838764 and 1142123) from the Division of Polar Programs. Partial support was provided by NSF-IGERT (0654336), Montana Space Grant Consortium and NSF-CDEBI (A.B.M); American Association of University Women, Montana Institute on Ecosystems, Start-up funding from Michigan Technological University (T.J.V-M); NSF-GRFP (A.M.A); Sêr Cymru National Research Network for Low Carbon, Energy and the Environment Grant from the Welsh Government and Higher Education Funding Council for Wales (A.C.M). We thank the WISSARD Science Team (wissard.org for list of members) for their assistance, B. Zook and J. Burnett (Deep SCINI) for GZ imagery, R. Scherer and R. Powell for sediment cores, and R. Vogt for comments. Logistics were provided by the 139th Expeditionary Airlift Squadron of the New York Air National Guard, Kenn Borek Air, and by the Antarctic Support Contractor, Lockheed-Martin. Hot water drill support was provided by the University of Nebraska-Lincoln, directed by F. Rack and D. Duling (chief driller), with D. Blythe, J. Burnett, C. Carpenter, D. Gibson, J. Lemery, A. Melby and G. Roberts. The authors also thank two anonymous reviewers for constructive comments. The data generated and analyzed in this study are deposited in the mARS database at <http://ipt.biodiversity.aq/resource.do?r=gbase>, and in the OpenFluor database under ID# 628 (links are not yet live, data were provided as supplement with original submission and will be live upon acceptance).

References

Achberger, A. M., Michaud, A. B., Vick-Majors, T. J., Christner, B. C., Skidmore, M. L., Priscu, J. C., & Tranter, M. (2017). Microbiology of Subglacial Environments, p. 83–110. *In* Psychrophiles: From Biodiversity to Biotechnology. Springer International Publishing.

- Achberger, A. M., Christner, B. C., Michaud, A. B., Priscu, J. C., Skidmore, M. L., & Vick-Majors, T. J. (2016). Microbial Community Structure of Subglacial Lake Whillans, West Antarctica. *Frontiers in Microbiology*. **7**, 256–13.
- Barker, J. D., Klassen, J. L., Sharp, M. J., Fitzsimons, S. J., & Turner, R. J. (2010). Detecting biogeochemical activity in basal ice using fluorescence spectroscopy. *Annals of Glaciology* **51**, 47–55.
- Bauer, J. E., Cai, W. J., Raymond, P. A., Bianchi, T. S., Hopkinson, C. S., & Regnier, P. (2013). The changing carbon cycle of the coastal ocean. *Nature*. **504**, 61–70.
- Beem, L. H., Jezek, K. C., & C. J. Van Der Veen. (2010). Basal melt rates beneath the Whillans Ice Stream, West Antarctica. *Journal of Glaciology*. **56**, 647-654.
- Begeman, C.B., Tulaczyk, S.M., Marsh, O.J., Mikucki, J.A., Stanton, T.P., Hodson, T.O., et al., (2018). Ocean stratification and low melt rates at the Ross Ice Shelf grounding zone. *Journal of Geophysical Research: Oceans*, **123**, (10), 7438-7452
- Bercovici, S. K., Huber, B. A., DeJong, H. B., Dunbar, R. B. & Hansell, D. A. (2017). Dissolved organic carbon in the Ross Sea: Deep enrichment and export. *Limnology and Oceanography*. **62**, 2593–2603.
- Berman, T., & Bronk, D. A. (2003). Dissolved organic nitrogen: a dynamic participant in aquatic ecosystems. *Aquatic Microbial Ecology*. **31**, 279–305.
- Bhatia, M. P., Kujawinski, E. B., Das, S. B., Breier, C. F., Henderson, P. B., & Charette, M. (2013). Greenland meltwater as a significant and potentially bioavailable source of iron to the ocean. *Nature Geoscience*. **6**, 274-278.
- Blythe, D. S., Duling, D. V. & Gibson, D. E. (2014). Developing a hot-water drill system for the WISSARD project: 2. In situ water production. *Annals of Glaciology* **55**, 298–302.
- Burdige, D. J., Alperin, M. J., Homstead, J., & Martens, C. S. (1992). The Role of Benthic Fluxes of Dissolved Organic Carbon in Oceanic and Sedimentary Carbon Cycling. *Geophysical Research Letters*. **19**, 1851–1854.
- Burnett, J., Rack, F. R., Blythe, D., Swanson, P., Duling, D., Gibson, D., et al., (2014). Developing a hot-water drill system for the WISSARD project: 3. Instrumentation and control systems. *Annals of Glaciology*. **55**, 303–310.
- Carlson, C. A., Bates, N. R., Ducklow, H. W. & Dennis, A. (1999). Estimation of bacterial respiration and growth efficiency in the Ross Sea, Antarctica. *Aquatic Microbial Ecology*. **19**, 229–244.
- Carter, S. P. & Fricker, H. A. (2012). The supply of subglacial meltwater to the grounding line of the Siple Coast, West Antarctica. *Annals of Glaciology*. **53**, 267–280.
- Chin-Leo, G. & Kirchman, D. L. (1988). Estimating bacterial production in marine waters from the simultaneous incorporation of thymidine and leucine. *Applied and Environmental Microbiology*. **54**, 1934–1939.
- Christianson, K., Anandakrishnan, S., Jacobel, R. W., Horgan, H. J., & Alley, R. B. (2012). Subglacial Lake Whillans — Ice-penetrating radar and GPS observations of a shallow active reservoir beneath a West Antarctic ice stream. *Earth and Planetary Science Letters*. **331-332**, 237–245.
- Christianson, K., Jacobel, R. W., Horgan, H. J., Alley, R. B., Anandakrishnan, S., Holland, D. M., & DallaSanta, K. J. (2016). Basal conditions at the grounding zone of Whillans Ice Stream, West Antarctica, from ice-penetrating radar. *Journal of Geophysical Research: Earth Surface*. **121**, 1954–1983. <http://doi.org/10.1002/2015JF003806>

- Christner, B. C., Royston-Bishop, G., Foreman, C. M., Arnold, B. R., Tranter, M., et al., (2006). Limnological conditions in Subglacial Lake Vostok, Antarctica. *Limnology Oceanography*. **51**, 2485–2501.
- Christner, B. C., Priscu, J. C., Achberger, A. M., Barbante, C., Carter, S. P., Christianson, K., et al., (2014). A microbial ecosystem beneath the West Antarctic ice sheet. *Nature*. **512**, 310–313.
- Christoffersen, P., Bougamont, M., Carter, S. P., Fricker, H. A. & Tulaczyk, S. (2014). Significant groundwater contribution to Antarctic ice streams hydrologic budget. *Geophysical Research Letters*. **41**, 2003–2010.
- Clough, J. W., & Hansen, B. L. (1979). The Ross Ice Shelf Project. *Science*. **203**, 433–434.
- Coble, P. G. (1996). Characterization of marine and terrestrial DOM in seawater using excitation-emission matrix spectroscopy. *Marine Chemistry*, **51**, 325–346.
- Cory, R. M., & McKnight, D. M. (2005). Fluorescence spectroscopy reveals ubiquitous presence of oxidized and reduced quinones in dissolved organic matter. *Environmental Science Technology*. **39**, 8142–8149.
- Cotner, J. B., Hall, E. K., Scott, J. T., & Heldal, M. (2010). Freshwater Bacteria are Stoichiometrically Flexible with a Nutrient Composition Similar to Seston. *Frontiers in Microbiology*. **1**, 132. <http://doi.org/10.3389/fmicb.2010.00132>
- Dai, M., Yin, Z., Meng, F., Liu, Q., Cai, W. J. (2012). Spatial distribution of riverine DOC inputs to the ocean: An updated global synthesis. *Current Opinion in Environmental Sustainability*. **4**, 170–178.
- Das, S. B., Joughin, I., Behn, M. D., Howat, I. M., King, M. A., Lizarralde, D., & Bhatia, M. P. (2008). Fracture propagation to the base of the Greenland Ice Sheet during supraglacial lake drainage. *Science*. **320**, 778–781.
- D'Andrilli, J., Foreman, C. M., Sigl, M., Priscu, J. C. & McConnell, J. R. (2017). A 21 000-year record of fluorescent organic matter markers in the WAIS Divide ice core. *Climate of the Past* **13**, 533–544.
- Dubnick, A., Barker, J., Sharp, M., & Wadham, J. (2010). Characterization of dissolved organic matter (DOM) from glacial environments using total fluorescence spectroscopy and parallel factor analysis. *Annals of Glaciology*. **51**, 111–122.
- Dubnick, A., Wadham, J., Tranter, M., et al. (2017). Trickle or treat: The dynamics of nutrient export from polar glaciers. *Hydrological Processes*. **31**, 1776–1789.
- Fisher, A. T., Mankoff, K. D., Tulaczyk, S. M., Tyler, S. W., Foley, N. & the WISSARD Science Team. (2015). High geothermal heat flux measured below the West Antarctic Ice Sheet. *Science Advances*. **1**, e1500093–e1500093.
- Foley, N., Tulaczyk, S. M., Grombacher, D., Doran, P. T., Mikucki, J., Myers, K. F. et al., (2019). Evidence for Pathways of Concentrated Submarine Groundwater Discharge in East Antarctica from Helicopter-Borne Electrical Resistivity Measurements. *Hydrology*. **6**, (2), 54.
- Fricker, H. A., & Scambos, T. (2009). Connected subglacial lake activity on lower Mercer and Whillans ice streams, West Antarctica, 2003–2008. *Journal of Glaciology*. **55**, 303–315.
- Fricker, H. A., Scambos, T., Bindshadler, R. & Padman, L. (2007). An active subglacial water system in West Antarctica mapped from space. *Science*. **315**, 1544–1548.
- Gonçalves-Araujo, R., Stedmon, C. A., Heim, B., Dubinenkov, I., Kraberg, A., Moiseev, D. & Bracher, A. (2015). From Fresh to Marine Waters: Characterization and Fate of Dissolved

- Organic Matter in the Lena River Delta Region, Siberia. *Frontiers in Marine Science*. **2**, 108. doi:10.3389/fmars.2015.00108
- Hawkings, J., J. Wadham, M. Tranter, Telling, J., Bagshaw, E., Beaton, A., Simmons, S.-L., Chandler, D., Tedstone, A. & Nienow, P. (2016). The Greenland Ice Sheet as a hot spot of phosphorus weathering and export in the Arctic. *Global Biogeochemical Cycles*. **30**, 191–210.
- Hodgson, D. A., Roberts, S. J., Bentley, M. J., Carmichael, E. L., Smith, J. A., Verleyen, E., et al., (2009). Exploring former subglacial Hodgson Lake, Antarctica. Paper II: palaeolimnology. *Quaternary Science Reviews*. **28**, 2310–2325.
- Hodson, T. O., Powell, R. D., Brachfeld, S. A., Tulaczyk, S., Scherer, R. P. & WISSARD Science Team. (2016). Physical processes in Subglacial Lake Whillans, West Antarctica: Inferences from sediment cores. *Earth and Planetary Science Letters*. **444**, 56–63.
- Hood, E., Battin, T. J., Fellman, J., & O'Neel, S. (2015). Storage and release of organic carbon from glaciers and ice sheets. *Nature Geoscience*. **8**, 91–96.
- Horgan, H. J., Alley, R. B., Christianson, K., Anandakrishnan, S., Horgan, H. J., Alley, R. B., et al., (2013). Estuaries beneath ice sheets. *Geology*. **41**. 1159–1162.
- Horgan, H. J., Anandakrishnan, S., Jacobel, R. W., Christianson, K., Alley, R. B., Heeszel, D. S., et al., (2012). Subglacial Lake Whillans — Seismic observations of a shallow active reservoir beneath a West Antarctic ice stream. *Earth and Planetary Science Letters*. **331**, 201–209.
- Horrigan, S. G. (1981). Primary production under the Ross Ice Shelf, Antarctica. *Limnology and Oceanography*. **26**, 378–382.
- Huguet, A., Vacher, L., Relexans, S., Saubusse, S., Froidefond, J. M., & Parlanti, E. (2009). Properties of fluorescent dissolved organic matter in the Gironde Estuary. *Organic Geochemistry*, **40**, 706–719.
- Kjær, H. A., Svensson, A., Vallelonga, P., Kettner, E., Schüpbach, S., Bigler, et al., (2011). First continuous phosphate record from Greenland ice cores. *Climate of the Past Discussions*. **7**, 3959–3989. <http://doi.org/10.5194/cpd-7-3959-2011>
- Kepner, R. L., Wharton, R. A., & Suttle, C. A. (1998). Viruses in Antarctic Lakes. *Limnology and Oceanography*. **43**, 1754–1761.
- Kirchman, D., K'nees, E. & Hodson, R. (1985). Leucine incorporation and its potential as a measure of protein synthesis by bacteria in natural aquatic systems. *Applied and Environmental Microbiology*. **49**, 599–607.
- Lambert, T., Bouillon, S., Darchambeau, F., Morana, C., Roland, F. A. E., Descy, J. P., & Borges, A. V. (2017). Effects of human land use on the terrestrial and aquatic sources of fluvial organic matter in a temperate river basin (The Meuse River, Belgium). *Biogeochemistry*, **136**, 191–211. <http://doi.org/10.1007/s10533-017-0387-9>
- Lawson, E. C., J. L. Wadham, M. Tranter, M. Stibal, G. P. Lis, C. E. H. Butler, J. Laybourn-Parry, P. Nienow, D. Chandler, and P. Dewsbury. (2014). Greenland Ice Sheet exports labile organic carbon to the Arctic oceans. *Biogeosciences*. **11**: 4015–4028.
- Lawson, J., Doran, P.T., Kenig, F. & Priscu, J.C. (2004). Stable carbon and nitrogen isotopic. *Aquatic Geochemistry*. **10**, (3-4), 269–301.
- Li, Y. and Gregory, S. (1974). Diffusion of ions in sea water and deep-sea sediments. *Geochimica Cosmochimica Acta*. **38**, 703–714.
- Meybeck, M. (1982). Carbon, nitrogen, and phosphorus transport by world rivers. *American Journal of Science*. **282**, 401–450.

- McKnight, D. M., Boyer, E. W., Westerhoff, P. K., Doran, P. T., Kulbe, T., & Andersen, D. T. (2001). Spectrofluorometric characterization of dissolved organic matter for indication of precursor organic material and aromaticity. *Limnology and Oceanography*. **46**: 38–48.
- Michaud, A. B., Dore, J. E., Achberger, A. M., Christner, B. C., Mitchell, A. C., Skidmore, M. L., et al., (2017). Microbial oxidation as a methane sink beneath the West Antarctic Ice Sheet. *Nature Geoscience*. **10**, 1–8.
- Michaud, A. B., Skidmore, M. L., Mitchell, A. C., Vick-Majors, T. J., Barbante, C., Turetta, C., et al., (2016). Solute sources and geochemical processes in Subglacial Lake Whillans, West Antarctica. *Geology*. **44**, 347–350.
- Mikucki, J. A., Pearson, A., Johnston, D. T., Turchyn, A. V., Farquhar, J., Schrag, D. P., et al., (2009). A Contemporary Microbially Maintained Subglacial Ferrous “Ocean.” *Science*. **324**, 397–400.
- Mikucki, J. A., Lee, P. A., Ghosh, D., Purcell, A. M., Mitchell, A. C., Mankoff, K. D., et al., (2016). Subglacial Lake Whillans microbial biogeochemistry: a synthesis of current knowledge. *Philosophical Transactions of the Royal Society A: Mathematical, Physical and Engineering Sciences*. 374, <https://doi.org/10.1098/rsta.2014.0290>.
- Murphy, K. R., Stedmon, C. A., Graeber, D. & Bro, R. (2013). Fluorescence spectroscopy and multi-way techniques. *PARAFAC. Analytical Methods*. **5**, 6557–11.
- Murphy, K. R., Stedmon, C. A., Wenig, P., & Bro, R. (2014). OpenFluor– an online spectral library of auto-fluorescence by organic compounds in the environment. *Analytical Methods*. **6**, 658–661.
- Muto, A., Christianson, K., Horgan, H. J., Anandakrishnan, S., & Alley, R. B. (2013). Bathymetry and geological structures beneath the Ross Ice Shelf at the mouth of Whillans Ice Stream, West Antarctica, modeled from ground-based gravity measurements. *Journal of Geophysical Research Solid Earth*. **118**, 4535–4546.
- Oswald, G. K., Rzvanbehbahani, S., & Stearns, L. A. (2018). Radar evidence of ponded subglacial water in Greenland. *Journal of Glaciology*. **64**, 711–729.
- Palmer, S. J., Dowdeswell, J. A., Christoffersen, P., Young, D. A., Blankenship, D. D., Greenbaum, J. S., et al., (2013). Greenland subglacial lakes detected by radar. *Geophysical Research Letters*. **40**, 6154–6159.
- Parlanti, E., Worz, K., Geo, L., & Lamotte, M. (2000). Dissolved organic matter fluorescence spectroscopy as a tool to estimate biological activity in a coastal zone submitted to anthropogenic inputs. *Organic Geochemistry*. **31**, 1765–1781.
- Porcal, P., Kopáček, J., & Tomková, I. (2014). Seasonal photochemical transformations of nitrogen species in a forest stream and lake. *PLoS ONE* **9**, e116364.
- Priscu, J. C., Achberger, A. M., Cahoon, J. E., Christner, B. C., Edwards, R. L., Jones, W. L., et al., (2013). A microbiologically clean strategy for access to the Whillans Ice Stream subglacial environment. *Antarctic Science*. **25**, 637–647.
- Priscu, J. C., Adams, E. E., Lyons, W. B., Voytek, M. A., Mogk, D. W., Brown, R. L., et al., (1999). Geomicrobiology of subglacial ice above Lake Vostok, Antarctica. *Science*. **286**, 2141–2144.
- Priscu, J. C., Tulaczyk, S., Studinger, M., Kennicutt II, M. C., Christner, B. C. & C. M. Foreman. (2008). Antarctic Subglacial Water: Origin, Evolution, and Ecology, p. 119–135. In W.F. Vincent and J. Laybourn-Parry [eds.], *Polar Lakes and Rivers*. Polar Lakes and Rivers.

- Purcell, A. M., Mikucki, J. A., Achberger, A. M., Alekhina, I. A., Barbante, C., Christner, B. C., et al., (2014). Microbial sulfur transformations in sediments from Subglacial Lake Whillans. *Frontiers in Microbiology*. **5**, 594.
- Rack, F. R., Duling, D., Blythe, D., Burnett, J., Gibson, D., Roberts, G. et al., (2014). Developing a hot-water drill system for the WISSARD project: 1. Basic drill system components and design. *Annals of Glaciology*. **55**, 285-297
- Raven, J. A. (1988). The iron and molybdenum use efficiencies of plant growth with different energy, carbon and nitrogen sources. *New Phytologist*. **109**: 279–288.
<http://doi.org/10.1111/j.1469-8137.1988.tb04196.x>
- Redfield, A. C., Ketchum, B. K. & Richards, F. A. (1963). The influence of organisms on the composition of sea-water, *In* Hill MN, editor. *The Sea*, Vol. II. pp. 26–77. John Wiley, New York.
- Rignot, E., Jacobs, S., Mouginot, J., & Scheuchl, B. (2013). Ice-shelf melting around Antarctica. *Science*. **341**, 266–270.
- Romera-Castillo, C., Sarmiento, H., Alvarez-Salgado, X. A., Gasol, J. M., & Marrase, C. (2011). Net Production and Consumption of Fluorescent Colored Dissolved Organic Matter by Natural Bacterial Assemblages Growing on Marine Phytoplankton Exudates. *Applied and Environmental Microbiology*. **77**, 7490–7498.
- Santibáñez, P.A., Maselli, O.J., Greenwood, M., Grieman, M.M., Saltzman, E.S., McConnell, J.R., & Priscu, J. C. (2018). Prokaryotes in the WAIS Divide ice core reflect source and transport changes between Last Glacial Maximum and the early Holocene. *Global Change Biology*. DOI: 10.1111/gcb.14042.
- Seeberg-Elverfeldt, J., Schlüter, M., Feseker, T., & Kölling, M. (2005). Rhizon sampling of porewaters near the sediment-water interface of aquatic systems. *Limnology and Oceanography Methods*. **3**: 361–371.
- Shen, L., & Chen. Z. 2007. Critical review of the impact of tortuosity on diffusion. *Chemical Engineering Science*. **62**, 3748–3755.
- Siegert, M. J., Ross, N., & Le Brocq, A. M. (2016). Recent advances in understanding Antarctic subglacial lakes and hydrology. *Philosophical Transactions of the Royal Society A: Mathematical, Physical, and Engineering Sciences*. **374**, 20140306.
- Siegfried, M. R., Fricker, H. A., Roberts, M., Scambos, T. A., & Tulaczyk, S. (2014). A decade of West Antarctic subglacial lake interactions from combined ICESat and CryoSat-2 altimetry. *Geophysical Research Letters*. **41**, 891–898.
- Siegfried, M. R., Fricker, H. A., Carter, S. P., & Tulaczyk, S. (2016). Episodic ice velocity fluctuations triggered by a subglacial flood in West Antarctica. *Geophysical Research Letters*. **43**, 2640–2648.
- Siegfried, M. R., & Fricker, H. A. (2018). Thirteen years of subglacial lake activity in Antarctica from multi-mission satellite altimetry. *Annals of Glaciology*. **59**, 42–55.
- Smethie, W. M., Jr. & Jacobs, S. S. (2005). Circulation and melting under the Ross Ice Shelf: estimates from evolving CFC, salinity and temperature fields in the Ross Sea. *Deep Sea Research Part I: Oceanographic Research Papers*. **52**, (6), 959-978.
[doi:10.1016/j.dsr.2004.11.016](http://doi.org/10.1016/j.dsr.2004.11.016)
- Smith, B. E., Tulaczyk, S., Fricker, H. A., & Joughin, I. R. (2009). An inventory of active subglacial lakes in Antarctica detected by ICESat (2003–2008). *Journal of Glaciology*. **55**: 573–595.

- Solórzano, L., & Sharp, J. H. (1980). Determination of total dissolved phosphorus and particulate phosphorus in natural waters. *Limnology and Oceanography*. **25**: 754–758.
- Statham, P.J., Skidmore, M. & Tranter, M. (2008). Inputs of glacially derived dissolved and colloidal iron to the coastal ocean and implications for primary productivity. *Global Biogeochemical Cycles*. **22**, GB3013, doi: 10.1029/2007GB003106.
- Stedmon, C. A., Markager, S., Bro, R. (2003). Tracing dissolved organic matter in aquatic environments using a new approach to fluorescence spectroscopy. *Marine Chemistry*. **82**, 239–254, [https://doi.org/10.1016/S0304-4203\(03\)00072-0](https://doi.org/10.1016/S0304-4203(03)00072-0).
- Strickland, J. D. H & Parsons, T. R. (1968). *A practical handbook of seawater analysis*. Ottawa: Fisheries Research Board of Canada.
- Takacs, C. D., Priscu, J. C. & McKnight, D. M. (2001). Bacterial dissolved organic carbon demand in McMurdo Dry Valley lakes, Antarctica. *Limnology and Oceanography*. **46**, 1189–1194.
- Tulaczyk, S., Mikucki, J. A., Siegfried, M. R., Priscu, J. C., Barcheck, C. G., Beem, L. H. et al., (2014). WISSARD at Subglacial Lake Whillans, West Antarctica: scientific operations and initial observations. *Annals of Glaciology*. **55**, 51–58.
- Turetta, C., Cozzi, G., Barbante, C., Capodaglio, G., & Cescon, P. (2004). Trace element determination in seawater by ICP-SFMS coupled with a microflow nebulization/desolvation system. *Analytical and Bioanalytical Chemistry*. **380**, 258–268.
- Vähätalo, A. V., & Zepp, R. G. (2005). Photochemical Mineralization of Dissolved Organic Nitrogen to Ammonium in the Baltic Sea. *Environmental Science and Technology*. **39**, 6985–6992.
- Vick-Majors, T. J., Achberger, A., Santibáñez, P. A., Dore, J. E., Michaud, A. B., Christner, B. C., et al., (2015). Biogeochemistry and microbial diversity in the marine cavity beneath the McMurdo Ice Shelf, Antarctica. *Limnology and Oceanography*. **61**, 572–586.
- Vick-Majors, T. J., Mitchell, A. C., Achberger, A. M., Christner, B. C., Dore, J. E., Michaud, A. B. et al., (2016). Physiological Ecology of Microorganisms in Subglacial Lake Whillans. *Frontiers in Microbiology*. **7**, 1457–16.
- Walker, S. A., Amon, R. M. W., & Stedmon, C. A. (2013). Variations in high-latitude riverine fluorescent dissolved organic matter: A comparison of large Arctic rivers. *Journal of Geophysical Research: Biogeosciences*. **118**:1689–1702. <http://doi.org/10.1002/2013JG002320>
- Wadham, J. L., Arndt, S., Tulaczyk, S., Stibal, M., Tranter, M., Telling, J., et al., (2012). Potential methane reservoirs beneath Antarctica. *Nature*. **488**, 633–637.
- Wadham, J. L., De'ath, R., Monteiro, F. M., Tranter, M., Ridgwell, A., Raiswell, R. & Tulaczyk, S. (2013). The potential role of the Antarctic Ice Sheet in global biogeochemical cycles. *Earth and Environmental Science Transactions of the Royal Society of Edinburgh*. **104**, 55–67.
- Wadham, J. L., Hawkings, J., Telling, J., Chandler, D., Alcock, J., O'Donnell, E. et al., (2016). Sources, cycling and export of nitrogen on the Greenland Ice Sheet. *Biogeosciences*. **13**, 6339–6352.
- Willis, M.J., Herried, B.G., Bevis, M.G. & Bell, R.E. (2015). Recharge of a subglacial lake by surface meltwater in northeast Greenland. *Nature*. **518**, 7538.
- Wilson, H. F. & Xenopoulos, M. A. (2009). Effects of agricultural land use on the composition of fluvial dissolved organic matter. *Nature Geoscience*. **2**, 37–41.

- 967 Wolff, E. W. (2013). Ice sheets and nitrogen. *Philosophical Transactions of the Royal Society of*
968 *London. Series B, Biological Sciences*. **368**, 20130127.
- 969 Wright, A., & Siegert, M. (2012). A fourth inventory of Antarctic subglacial lakes. *Antarctic*
970 *Science*. **24**, 659–664.
- 971 Zehr, J. P., Paulsen, S. G., Axler, R. P., & Goldman, C. R. (1988). Dynamics of dissolved
972 organic nitrogen in subalpine Castle Lake, California. *Hydrobiologia*. **157**, 33–45.
973